

Copyright © 1964, by the author(s).  
All rights reserved.

Permission to make digital or hard copies of all or part of this work for personal or classroom use is granted without fee provided that copies are not made or distributed for profit or commercial advantage and that copies bear this notice and the full citation on the first page. To copy otherwise, to republish, to post on servers or to redistribute to lists, requires prior specific permission.

Electronics Research Laboratory  
University of California  
Berkeley, California  
Internal Technical Memorandum M-97

ELECTRICAL DIPOLE INVERSION IN RUBY  
EXCITED BY A COHERENT LIGHT SOURCE

by

I. F. Roberts

The research herein was sponsored by the U. S. Army  
Research Office Durham under Grant DA-ARO-D-31-124-  
G-317.

August 27, 1964

## TABLE OF CONTENTS

ABSTRACT. . . . .	iv
I. INTRODUCTION . . . . .	1
A. General . . . . .	1
B. The laser . . . . .	1
C. Ruby as a laser material . . . . .	2
D. Laser action in ruby. . . . .	4
II. ELECTRICAL DIPOLE INVERSION IN RUBY . . . . .	5
A. General . . . . .	5
B. Transition probability in ruby. . . . .	5
C. Electrical dipole inversion . . . . .	7
D. Numerical calculations pertaining to dipole inversion . . . . .	10
III. EXPERIMENTAL PROCEDURE . . . . .	12
IV. RESULTS . . . . .	14
A. Uncoated rods . . . . .	14
B. Coated rods . . . . .	15
V. CONCLUSIONS. . . . .	15
REFERENCES . . . . .	16

## ACKNOWLEDGMENTS

The author wishes to express his gratitude to Professor J. R. Singer for the suggestion of this work, and also for his encouragement and guidance. Also he would like to express his thanks to his colleagues, A. S. Pine and L. H. C. Lin for invaluable help and stimulating discussions.

## ABSTRACT

The first section provides a simple introduction to the origin and development of the laser, with a brief description of how laser action occurs in ruby. Sec. II is devoted to a brief description of the theory of electrical dipole inversion in ruby; the important equations governing the theory are noted. Sec. III then deals with the experimental setup in detail, and Sec. IV describes and discusses the results.

## I. INTRODUCTION

### A. GENERAL

The use of stimulated emission for microwave amplifiers was proposed independently by Weber<sup>1</sup> at the University of Maryland; and Gordon Zeiger and Townes<sup>2</sup> at Columbia University. Ever since these microwave amplifiers (masers)\* were built, there was considerable expectation that the possibility of amplification and generation could be extended into the optical region.

In 1958, Schawlow and Townes<sup>3</sup> proposed the optical maser (or laser),\*\* and the first successful operation of such a laser was made by Maiman<sup>4</sup> in 1960. Since that time, considerable progress has been made in the understanding and development of the laser. A possibility quickly put forward was that the laser could be employed for communications. The suggestion was that the useful communication band would be extended into the sub-millimeter wavelength region.

A great deal of research has been carried out investigating and developing new materials, both solid state and gaseous, that exhibit laser action. Probably, the best known solid-state material thus far used is ruby, which Maiman used in his breakthrough experiment. Schawlow<sup>5</sup> had previously pointed out that stimulated emission in the  $R_1$  ruby line would be difficult to produce, because this line terminates in the ground state. However, there is a more complex energy band structure which causes laser operation in ruby.

### B. THE LASER

The laser by definition is a device that amplifies light by means of stimulated emission of radiation. It produces a beam of coherent

---

\* maser - microwave amplification by stimulated emission of radiation.

\*\* laser - light amplification by stimulated emission of radiation.

electromagnetic radiation having a particular well-defined frequency in that region of the spectrum broadly described as optical. This range includes the near ultraviolet, the visible and the infrared. The term coherence is to be emphasized because it is that property which distinguishes laser radiation from ordinary optical beams. On account of its coherence, a laser has remarkable properties; e. g., extremely high-energy density, a highly directional beam, extremely small divergence. These properties set the laser apart from ordinary light, which is incoherent.

Practically, a laser is generally used as a generator of radiation. The generator is constructed by the addition of a feedback mechanism in the form of mirrors to a light amplifier.

### C. RUBY AS A LASER MATERIAL

Fluorescence (noise) and stimulated emission in ruby can be understood with the aid of the energy level diagram (Fig. 1).

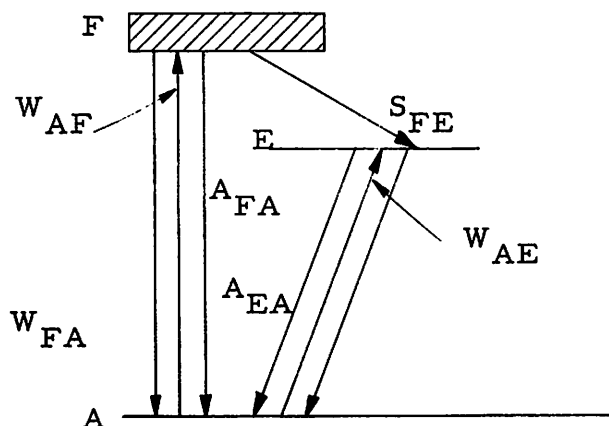


Fig. 1. Energy level diagram for a three-level fluorescent solid. (Stimulated transitions are indicated by W; spontaneous radiative transitions by A; and spontaneous nonradiative transitions by S.)

The ground state is denoted by index A. Excitation is supplied to the ruby by radiation of frequencies which produce absorption in the upper (F) band. Most of the absorbed energy is then transformed to the E level by radiationless transitions. The emission of radiation which gives rise to fluorescence is the spontaneous return from the E level to the ground (A) level. Fluorescence will take place at a low level of excitation. When the exciting radiation is sufficiently intense, it is possible to obtain more atoms (or molecules) in the E level than there are at the ground level.\* This gives rise to the stimulated emission and amplification. Stimulated emission will take place when the population of the ground level is greater than that of the E level, but the stimulated absorption will be greater than the emission, resulting in a loss of the number of photons, i. e., attenuation and not amplification occurs.

Incoherent fluorescence can be described as a cause of inefficiency because it is a drain on the E level population. In ruby, the lifetime of the E level is about 3 msec.<sup>6</sup> Therefore, on exciting the ruby by a light flash, no laser output is obtained for the energy required to excite a certain number of the atoms from the ground (A) level. Laser action is possible then only if the ruby can be placed in a condition of amplification (negative absorption) and a feedback situation is established by means of reflections. Negative absorption occurs in a stationary nonequilibrium state that depends on the rate at which excitation is provided, and also on the rate of relaxation and transitions, stimulated and spontaneous, that govern the passage of atoms through the cycle (Fig. 1). Generally, it is necessary that the rate of radiationless transfer from the uppermost level to the level at which the laser action begins, be fast compared to the other spontaneous transition rates.

---

\* Actually, the weighting factor is ignored here for simplicity. In fact, the weighting factor is important to ruby-laser action.



#### D. LASER ACTION IN RUBY

The energy level diagram for ruby is shown in Fig. 2. (Taken from the work of Sugano and Tanabe.<sup>7</sup>) The essential features of the energy diagram are the two wide (absorption) bands  ${}^4F_1$  and  ${}^4F_2$  and the split  ${}^2E$  level. Fluorescence in a ruby crystal can be demonstrated by irradiating the crystal with green light to excite the  ${}^4A_2 \rightarrow {}^4F_2$  transition and violet light to excite the  ${}^4A_2 \rightarrow {}^4F_1$  transition.

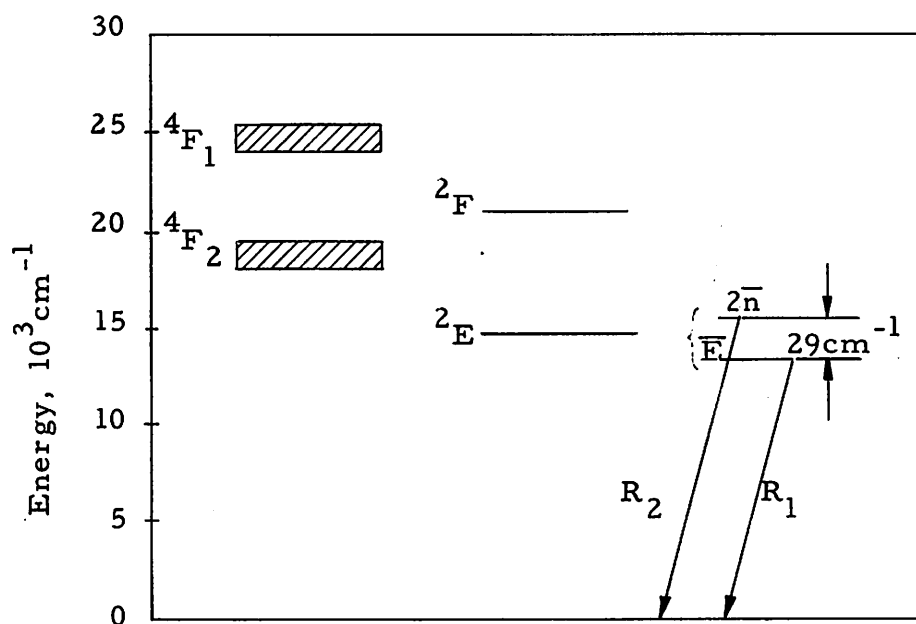


Fig. 2. Energy level diagram of ruby.

The emission spectrum at  $300^\circ\text{K}$  consists of two lines;  $R_1$  at  $6943 \text{ \AA}$  which is shown in Fig. 2 as originating from the  ${}^2\bar{E}$  level and the  $R_2$  line at  $6929 \text{ \AA}$  originating from the  ${}^2\tilde{E}$  level. Both lines terminate on the ground state  ${}^4A_2$ . The laser emission usually observed is due to the  $R_1$  transition at  $6943 \text{ \AA}$ . The  $R_1$  and  $R_2$  lines have half-power spectral widths of 4 and  $3 \text{ \AA}$  respectively at  $300^\circ\text{K}$ <sup>6</sup>, and a fluorescence line width of  $\sim 11 \text{ cm}^{-1}$  at  $300^\circ\text{K}$  and  $\sim 0.1 \text{ cm}^{-1}$  at  $77^\circ\text{K}$ <sup>8</sup>.

## II. ELECTRICAL DIPOLE INVERSION IN RUBY

### A. GENERAL

Singer and Wang<sup>9, 10</sup> proposed the theory that amplitude modulation of the output signal from a Quantum Mechanical Amplifier is to be expected for all maser oscillators except those in which the excited atoms are supplied at a notably greater rate than the depopulation rate due to coherent induced emission. They also suggest that an energy population inversion of electrical dipole moments can be performed using coherent light sources in the same manner as with magnetic dipole moments. Modulation of lasers may be accomplished by varying the population of excited states through control of the pumping energy.

If a secondary source is excited by a coherent light source, i. e., a laser; it seems feasible that under favorable alignment conditions, modulation of the output beam of the secondary source with respect to the input beam should be expected. The purpose of this project is to investigate whether such modulation occurs.

### B. TRANSITION PROBABILITY IN RUBY

For transitions between states  $n$ , and state  $m$ , where  $n$  is the lower state and  $m$  the upper state, the well-known Einstein spontaneous transition probability coefficient  $A_{nm}$  per atom of a transition in unit time, for an atom in state  $n$  is given by,<sup>11</sup>

$$A_{nm} = \frac{6\pi^2 g}{3h \lambda^3} |\mu_{nm}|^2 \quad (1)$$

where  $g$  is the degeneracy = 2 for ruby.<sup>8</sup>

$|\mu_{nm}|$  is the dipole moment matrix for the transition concerned defined by

$$\mu_{nm} = e \int_V \psi_m^* \mathbf{r} \psi_n dV \quad (2)$$

$\psi_n, \psi_m$  are the wave functions for the states  $n, m$ , respectively and  $\mathbf{r}$  is the radius vector.

In ruby, the most popular transition is that giving rise to the  $R_1$  line ( $6943 \text{ \AA}$ ), and  $A_{nm}$  becomes

$$A = 1.873 \times 10^{42} |\mu|^2.$$

The spontaneous emission lifetime  $\tau_{\text{spont}}$  is defined as

$$\tau_{\text{spont}} = \frac{1}{\sum A_{nm}}. \quad (3)$$

For ruby  $\tau_{\text{spont}} \cong 3 \text{ msecs.}^6$

Then the Einstein spontaneous-transition probability coefficient

$$A = \frac{1}{\tau_{\text{spont}}} \cong 330/\text{sec}.$$

From Eq. (1), then

$$\mu = 1.35 \times 10^{-20} \text{ e.s.u.}$$

The loss mechanisms are usually characterized in the single parameter  $t_{\text{photon}}$ , which is equal to the decay time constant of the radiation in a given mode presuming the amplifying medium is rendered neutral; i.e., population of the upper state is equal to the population of the lower state.  $t_{\text{photon}}$  is related to the total loss per pass  $\alpha$  (for simplicity, we assume the two mirrors at each end of the rod to be identical) and to the conventionally used quality factor 'Q' by

$$t_{\text{photon}} = \frac{L}{\alpha c} = \frac{Q}{2\pi V} \quad (4)$$

where  $c$  is the velocity of light in the medium, and  $L$  is the distance between mirrors. Eq. (4) is valid only for  $\alpha \ll 1$ .

Assuming  $\alpha = 0.05$  (five percent loss per pass) and  $L = 7.5 \text{ cms.}$ , then

$$t_{\text{photon}} \approx 0.8 \times 10^{-8} \text{ secs.}$$

This parameter may be increased by making  $\alpha$  smaller. The losses may be reduced by depositing an anti-reflection coating on one end of the ruby rod. If  $\alpha$  is reduced to 0.02 say, then

$$t_{\text{photon}} \approx 1.25 \times 10^{-8} \text{ secs.}$$

### C. ELECTRICAL DIPOLE INVERSION

The superposition state of a molecule may be described by the wave function

$$\psi = c_1 \psi_1 + c_2 \psi_2$$

The molecules are assumed to exist in one of two possible non-degenerate energy states,  $E_1$  the lower, and  $E_2$  the upper energy level.  $|c_1|^2$  is the probability that an atom (or molecule) is in the lower energy level and  $|c_2|^2$  is the probability of its being in the upper energy level. Both  $c_1$  and  $c_2$  are functions of time since the molecules make transitions between the states. For a two-state system, the wave functions may be simplified by determining the time dependence explicitly. In particular, the wave function of a system in a single state initially (suppose  $\psi_1$ ) is

$$u_1 \exp(iE_1 t)/\hbar = u_1 \exp(i\omega_1 t)$$

neglecting the phase of the wave which turns out to be of no importance in the final result.

The perturbation formula for a time rate of change of the coefficients of a set of wave functions is<sup>12</sup>

$$\dot{a}_n(t) = -\frac{i}{\hbar} \sum a_m(t) \int \psi_m^* H' \psi_n d\tau \quad (5)$$

where many states exist.

Here, only two states are of interest; the molecular system may be in only one or the other of these states. The perturbation energy  $H'$  is similar to a dipole interacting with an electric field.

If  $E = (0, 0, E_z \cos \omega t)$ , the perturbation energy is

$$H' = \vec{\mu} \cdot \frac{1}{2} \int_V E_z (e^{i\omega t} + e^{-i\omega t}) dV. \quad (6)$$

Considering transitions at a single frequency with the molecules entirely in the upper state  $u_2$  initially, i.e.,  $c_1 = 0$ ,  $c_2 = 1$ , then

$$\dot{c}_1(t) = -\frac{i}{\hbar} \int_V u_2^* \exp(-i\omega_2 t) \frac{1}{2} E_z (\exp(i\omega t) + \exp(-i\omega t)) u_1 \exp(i\omega_1 t) d\tau.$$

Defining the matrix element  $\mu_{\alpha 1} = \int_V u_\alpha^* r u_1 d\tau$  then

$$\dot{c}_1 = \frac{-i\mu_{21} E_z C_2 \omega_{21}}{2\hbar\omega} \exp(-i(\omega_{21} - \omega)t) \quad (7)$$

where  $\omega_{21} = \omega_2 - \omega_1 > 0$ , the term in  $(\omega_{21} + \omega)$  being ignored and  $\mu_{11}$  is zero.

Written in matrix form, then

$$\begin{bmatrix} \dot{c}_1 \\ \dot{c}_2 \end{bmatrix} = \frac{-i\mu_{21} E_z \omega_{21}}{2\hbar\omega} \begin{bmatrix} c_2 \exp(-i(\omega_{21} - \omega)t) \\ c_1 \exp(i(\omega_{21} - \omega)t) \end{bmatrix} \quad (8)$$

Defining  $r_1 = (c_1^* c_2 + c_2^* c_1)$

$$r_2 = i[c_1^* c_2 - c_2^* c_1]$$

$$r_3 = (c_2^* c_2 - c_1^* c_1)$$

then it can be shown<sup>13</sup> that the energy equation of such a system leads to a travelling-wave equation of the form

$$\frac{\partial^2 v}{\partial t^2} + \frac{c \partial^2 v}{\partial x \partial t} = -r^2 \sin v \quad (9)$$

where  $v = \frac{\mu_{21}}{\hbar} \int_0^t E_z dt$

and  $\Omega^2 = \frac{\pi}{\epsilon_0} N_e \hbar \omega_{21} \left( \frac{\mu_{21}}{\hbar} \right)^2$  where  $N_e$  = electron density.

For a standing wave,  $\partial/\partial x = 0$ .

Solution of Eq. (9) will yield equations in elliptic form and

$$\left. \begin{aligned} E_z &= E_z(0) \operatorname{dn} \left( \frac{r_0 t}{2}, k \right) & \text{for } k^2 < 1 \\ &= E_z(0) \operatorname{cn} \left( \frac{kr_0 t}{2}, k \right) & \text{for } k^2 > 1 \\ &= E_z(0) & \text{for } k^2 = 1 \end{aligned} \right\} \quad (10)$$

where

$$\Omega_0^2 = \frac{\mu_{21} E_z(0)}{\hbar} \quad \text{and} \quad k^2 = \frac{4\Omega^2}{\Omega_0^2}$$

Similarly,

$$\left. \begin{aligned} r_3 &= \frac{-N_e}{N_i} \left[ 1 - 2 \operatorname{Sn}^2 \left( \frac{r_0 t}{2}, k \right) \right] & k^2 < 1 \\ r_3 &= \frac{-N_e}{N_i} \left[ 1 - \frac{2}{k^2} \operatorname{Sn}^2 \left( \frac{kr_0 t}{2}, \frac{1}{k} \right) \right] & k^2 > 1 \\ r_3 &= \frac{-N_e}{N_i} \left[ 1 - 2 \tanh^2 \frac{r_0 t}{2} \right] & k^2 = 1 \end{aligned} \right\} \quad (11)$$

where  $N_i$  = ion density.

As these results are for the ideal case of a standing wave, they will not be discussed further.

A solution of the travelling wave can be found,<sup>13</sup> and to a first approximation

$$u(\lambda, \sigma) = u(0, \sigma) - \left[ \int_0^\lambda \sin \int_0^\sigma u(0, \sigma') - \int_0^{\lambda'} \sin \int_0^{\sigma'} u(0, \sigma'') \right. \\ \left. - \int_0^{\lambda^4} \dots \dots \right] d\sigma'' d\sigma' d\lambda' d\lambda \quad (12)$$

$$\text{where } \lambda = \frac{r^2(x)}{r_0^2} \left( \frac{r_0 x}{c} \right)$$

$$\text{and } \sigma = (t - \frac{x}{c}) r_0$$

This result is in the form of that given by Singer and Wang.<sup>10</sup> It is valid only when the photon density  $\gg$  two-state system density.

Also if  $\int_0^\sigma u(\lambda', \sigma') d\sigma' \ll 1$ , then it can be shown that the solution is a zero-order Bessel function, solution., i.e.,

$$u(\lambda, \sigma) = J_0(2\sqrt{\lambda\sigma}). \quad (13)$$

We thus have a description of the field variation at the output of the secondary source. The Bessel function plot is given in Fig. 3.

#### D. NUMERICAL CALCULATIONS PERTAINING TO DIPOLE INVERSION

$$\mu_{21} = 1.35 \times 10^{-20} \text{ e. s. u.}$$

$$\lambda = 6943 \text{ \AA}$$

$$\omega_{21} = 2.72 \times 10^{15} \text{ c/s}$$

$$\hbar\omega_{21} = 2.89 \times 10^{-12} \text{ ergs}$$

$$\tau_{\text{life}} = 3 \times 10^{-3} \text{ secs}$$

$$\tau_{\text{pulse}} = 2 \times 10^{-8} \text{ secs}$$

$$\begin{array}{l} \text{refractive} \\ \text{index } n \end{array} = 1.76$$

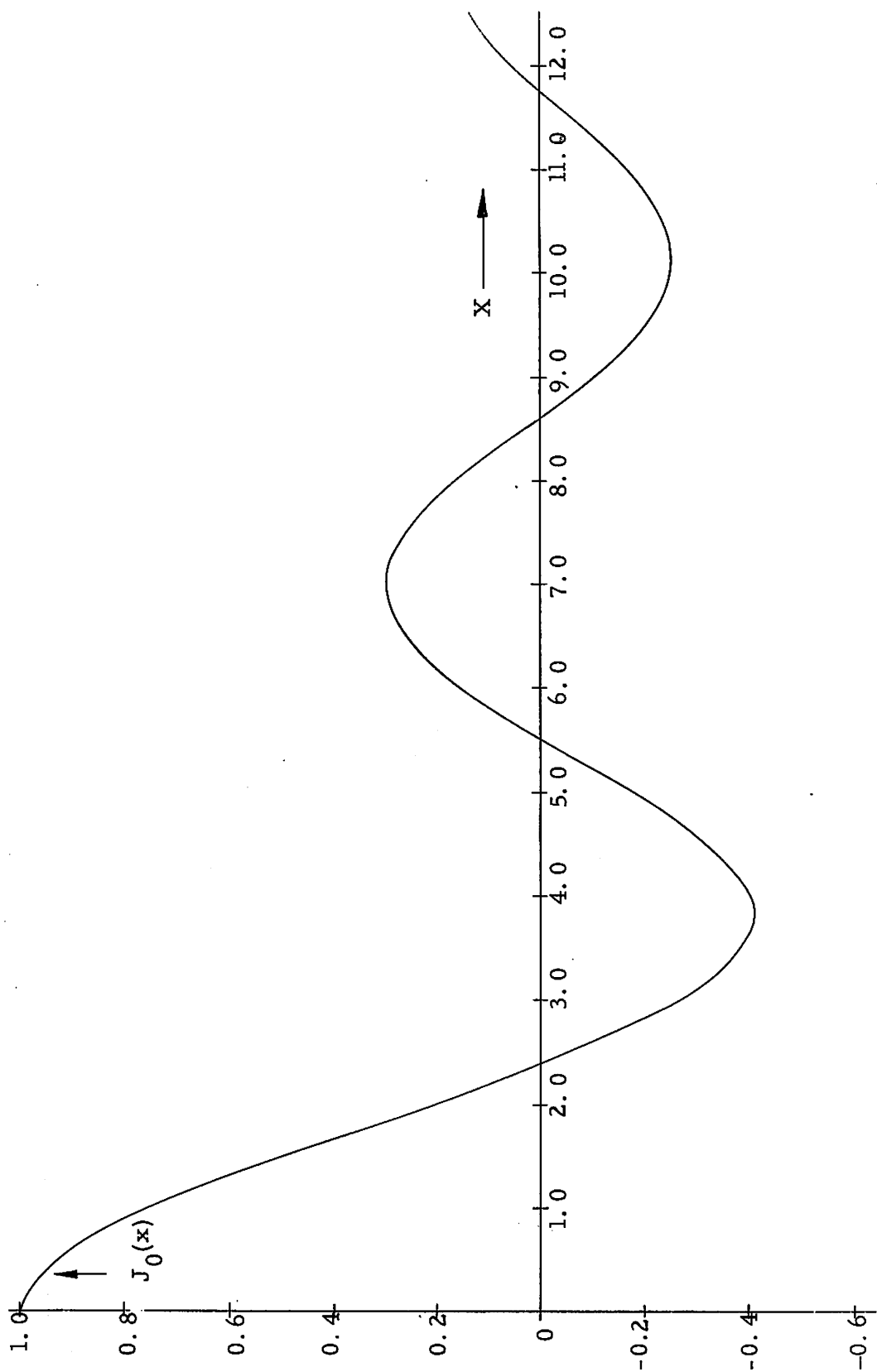


Fig. 3. Plot of Bessel function of zero order.



$$N_e = 5 \times 10^{18} / \text{cm}^3$$

$$\text{area of rod} = 0.3 \text{ cm}^2$$

$$L = 7.5 \text{ cm}$$

The power flow per unit area per unit time

$$\vec{S} = \frac{ce|\mathbf{E}|^2}{4\pi} = \frac{N_e \hbar \omega_{21}}{\tau_{\text{pulse}} \times \text{area}}$$

$$\text{Then } r_0 = \frac{\mu_{21} E(0)}{\hbar} = 9.62 \times 10^9 / \text{sec}$$

$$r^2(x) = \frac{\pi}{\epsilon} N_e(x) \hbar \omega_{21} \frac{\mu_{21}^2}{\hbar}$$

$$\text{and } N_e(x) = N_{2-1} \text{ per unit volume}$$

$$\therefore r = 3.4 \times 10^{10} / \text{sec}$$

$$k = \frac{2r}{r_0} \cong 7$$

Therefore, the frequency of the modulation pulse (due to dipole inversion) is of the order of  $10^{10}$  c/s.

Singer and Wang<sup>9</sup> showed that the equation governing the exchange of energy between molecules and the radiation is

$$\frac{\partial^2 E_2}{\partial t^2} + \frac{\omega E_z^2}{2Q} = 4\pi F N_e \hbar \omega_{21} \frac{0}{\partial t} \cos^2 \int_0^t \frac{\mu_{21} E(t') dt'}{\hbar} \quad (14)$$

where the integral of  $E(t)$  over time is needed to account for the variation of  $E$  with emission.

An approximate solution of Eq. (14) yields,<sup>9</sup>

$$\omega_1 \approx \frac{\mu_{21}}{\hbar} \left[ FN_e \hbar \omega_0 \right]^{1/2}$$

where  $F$  is the filling factor.

With  $F = 0.8$

$$\omega_1 = 4.5 \times 10^{10} \text{ c/s.}$$

This is in very close agreement with the calculations described here.

### III. EXPERIMENTAL PROCEDURE

The modulation frequency due to electrical dipole inversion is very high and will be extremely difficult to detect on the very best oscilloscope. An attempt was made to detect this frequency with a conventional oscilloscope as no travelling wave oscilloscope was available.

The block diagram of the experimental setup is shown in Fig. 4.

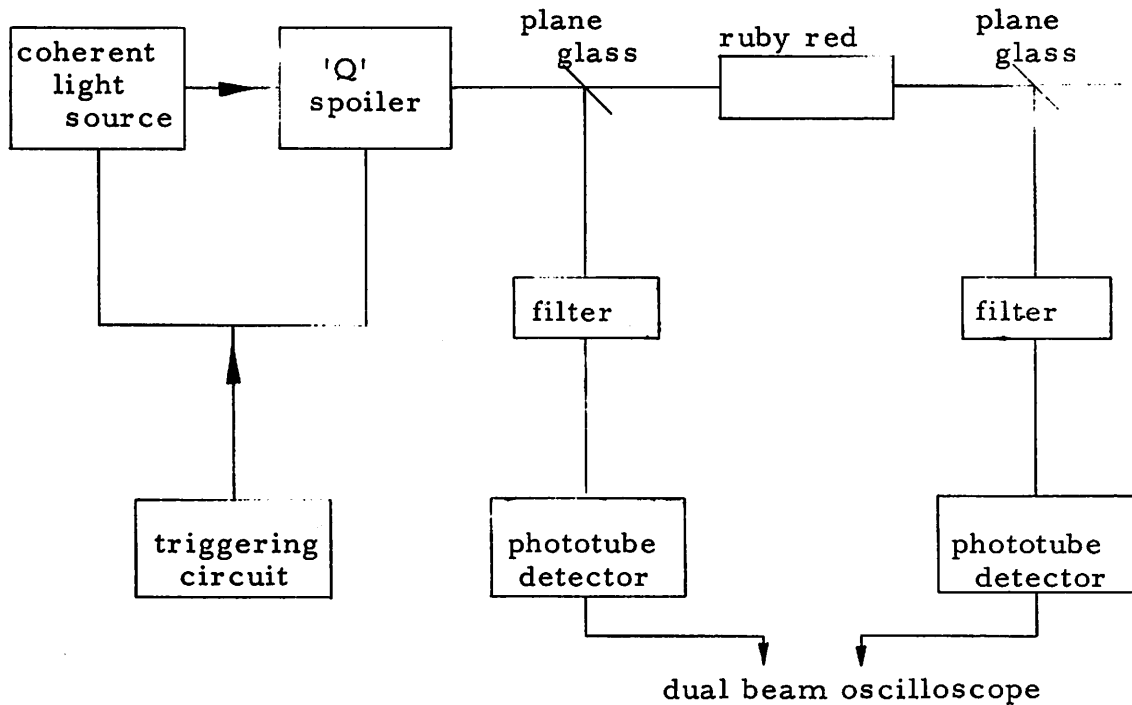


Fig. 4. Block diagram of the experimental system.

The coherent light (laser) source has a 'Q' spoiler attached directly to it. The purpose of the 'Q' spoiler is to lump the irregular pulsations of the ordinary ruby laser into one giant pulse. The particular model used in this experiment was a Lear-Siegler product giving an output pulse with peak power of 1Mw, and generally in the range 0.1 to 1.0Mw. The giant pulse emitted as a laser beam is divided by a glass plate positioned at  $45^{\circ}$ , thus allowing most of the power concentrated in the beam to activate the ruby. The beam is suitably filtered and detected, and the pulse recorded and photographed on one beam of the dual-beam oscilloscope.

The beam activating the ruby rod, causes electrical dipole inversion to occur, and in a similar manner to that described above the pulse after passing through the ruby rod is recorded and photographed. The two pulses are recorded and photographed simultaneously using Polaroid 10,000 film.

The two pulses were made identical in the absence of the rod that was to be energized. (The two pulses were identical in shape but varied in amplitude, as expected, due to the slight difference in intensity of the beam at each phototube.) Equalization was carried out by varying the balance levels of the oscilloscope preamplifiers. The rod was then placed in position and results duly recorded. These results will be discussed in the next section.

To improve the loss factor  $\alpha$ , it was decided to deposit an anti-reflection coating on one end of the ruby rods. Use was made of an existing vacuum system designed for such work and a suitable detection system was designed. (I am greatly indebted to L. H. C. Lin for the design of the phase detector.) For optimum performance, the coating was made a quarter wavelength thick. The detection system shown in Fig. 5, operates briefly as follows;

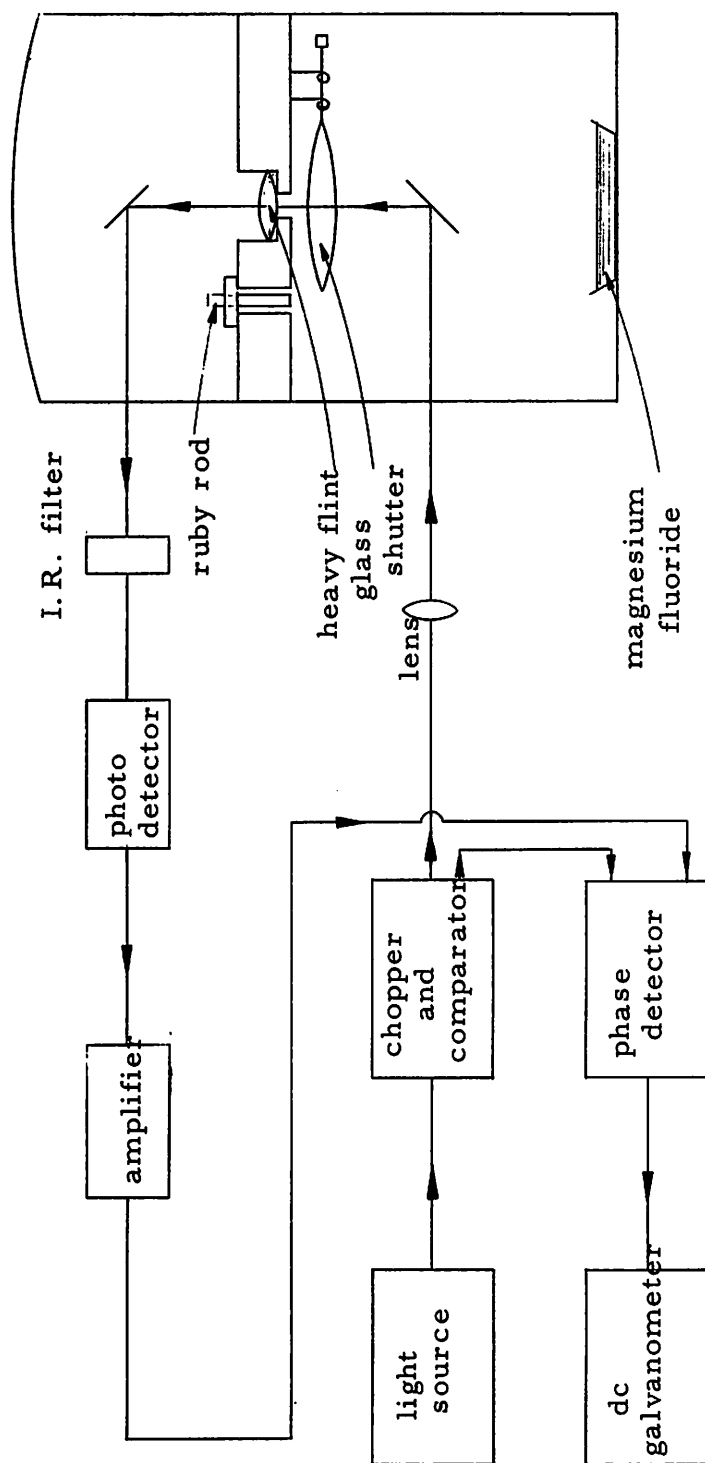


Fig. 5. Block diagram of system used to coat a ruby red.

The chopper consists of a rotating disc having grooves cut in it at equal intervals, thus sending square wave pulses (of a high enough frequency, so as to appear as a continuous light beam) along to the ruby rod that was to be coated. The comparison signal was obtained by means of a photo diode placed on one side of the rotating disc, and having a constant light source on the other side. The signal was then fed into the phase detector.

The light beam passes through the flint glass (having a refractive index of 1.79) and then via the infrared filter (to cut out laboratory light) into the photo detector. The signal was amplified and passed to the phase detector. The two signals were compared and the output signal recorded on a center null galvanometer.

The coating material used was magnesium fluoride ( $\text{MgF}_2$ ) having a comparable refractive index coefficient to that of ruby. A shutter operated externally by a magnet was placed between the ruby rod (and flint glass window) and the boat containing the  $\text{MgF}_2$ . Having pumped down the vacuum system ( $\leq 10^{-5}$  cms. Hg), the  $\text{MgF}_2$  was heated to vaporization. The shutter was moved to one side and a coating deposited on both the rod and glass window. This caused a change of output on the galvanometer, and by practice, one could obtain a maximum reading. This maximum reading corresponded to a quarter wavelength thickness of deposit--the required amount. The shutter was swung back thus completing the process.

Rods coated in such a manner were tested for dipole inversion as previously described.

## IV. RESULTS

### A. UNCOATED RODS

A series of tests were carried out with different ruby rods in an attempt to detect the modulation of the incoming pulse. Rods were used having their 'c' axis rotated through  $90^\circ$ , and others with zero-degree rotation of the 'c' axis.

The power input into the rod was varied by attenuating the intensity of the input light beam by means of neutral density filters.

The rods were rotated through  $180^\circ$ , in an attempt to detect the modulation.

Results show as can be seen from Figs. 6-11, that the only observable change was that of the amplitude of the pulse. This amplitude change remained unaltered at different power levels. Increase of the laser beam firing voltage level had the same effect.

## B. COATED RODS

It is difficult to say whether coating the rods did in fact cut down on the losses. However, results were found to be almost identical to those of the uncoated rods, and it seems superfluous to record two identical sets of results in this report.

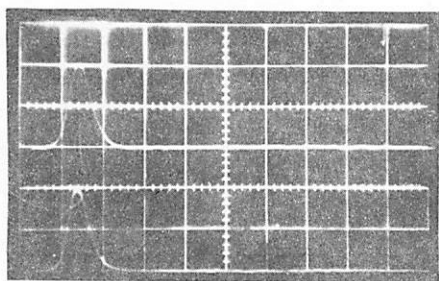
For this reason, the only set shown are those results for the uncoated rods, with Figs. 12 and 13 examples of pulses of the coated rods.

## V. CONCLUSIONS

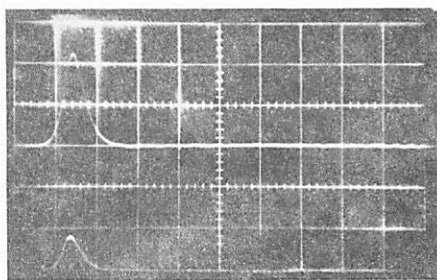
Theoretical studies briefly described in Sec. II. show that modulation of the output of a coherent light source after passing through a secondary source is feasible and is in agreement with the work of Singer and Wang.<sup>9, 10</sup>

The modulation frequency has been calculated to be of the order of 10 kMc/s--a very high frequency to detect by conventional means. Results using a dual-beam Tektronix (Type 551) oscilloscope with a time-scale range of  $2 \times 10^{-8}$  secs, and Type 925 phototubes failed to detect the modulation.

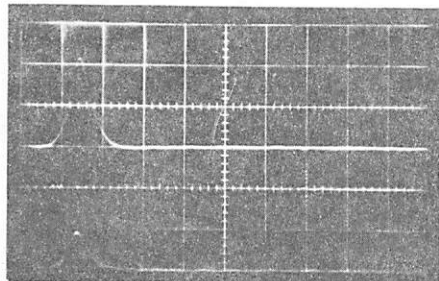
A more sensitive and faster detecting system will have to be developed (the use of a travelling wave oscilloscope etc.), before the modulation of the light beam may be seen.



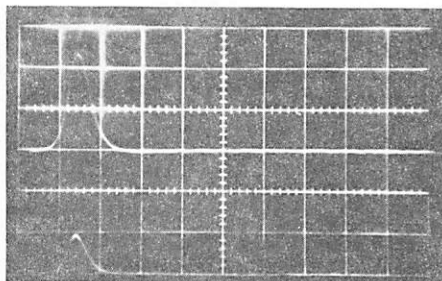
(a) No rod.



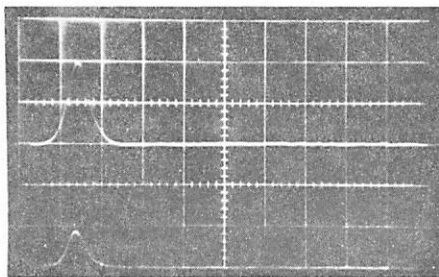
(b) Rod inserted - 70 filter.



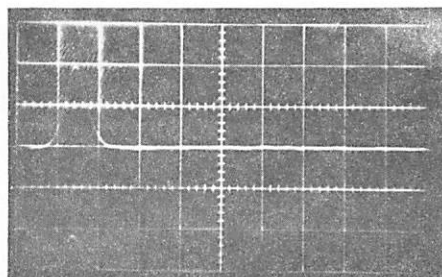
(c) N. D. 1.0 filter.



(d) N. D. 2.0 filter.

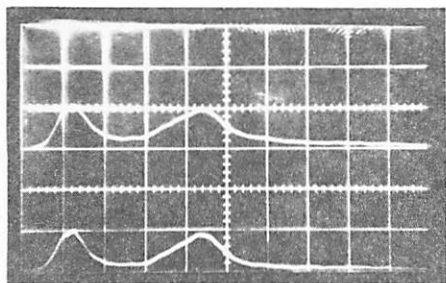


(e) N. D. 3.0 filter.

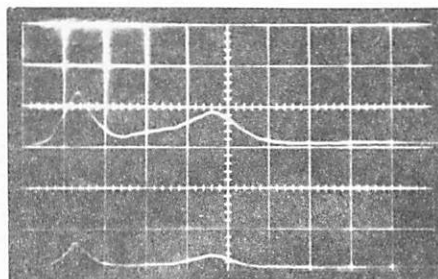


(f) N. D. 4.0 filter.

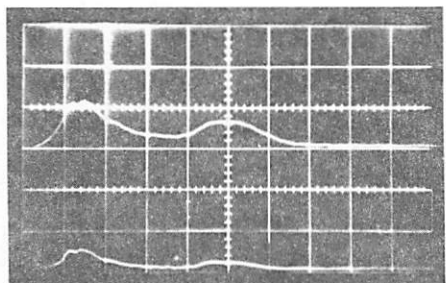
Fig. 6.  $0^\circ$  rotation of 'c' axis of ruby. Firing voltage of laser source 3800 V. (All curves are on a time scale of  $0.1 \mu$  secs/cm and 0.005 V/cm. N. D. 1.0. implies an attenuation factor of  $10^1$ . N. D. 2.0 implies an attenuation factor of  $10^2$ , etc. Note also that N. D. 3.0 filter for example means N. D. 3.0 at the 'Q' spoiler, and N. D.  $4.0 - 3.0 = 1.0$  at phototube detector. This manner of recording is used throughout the results.)



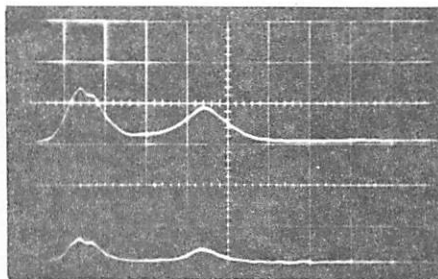
(a) No rod.



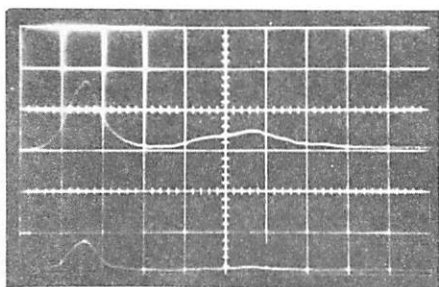
(b) Rod inserted - no filter.



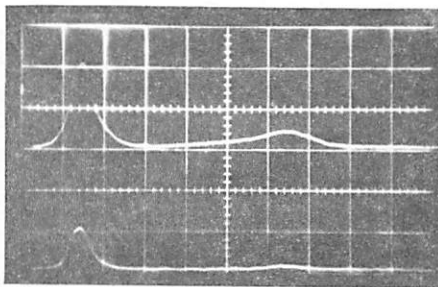
(c) N.D. 1.0 filter.



(d) N.D. 2.0 filter.



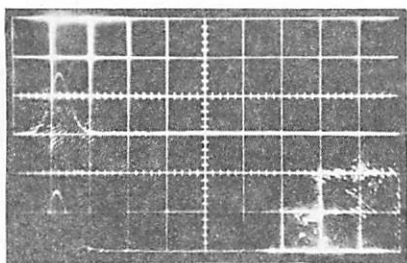
(e) N.D. 3.0 filter.



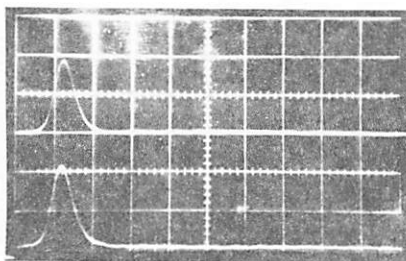
(f) N.D. 4.0 filter.

Fig. 7.  $0^\circ$  rotation of the 'c' axis of ruby. Firing voltage of laser source 3900 V.

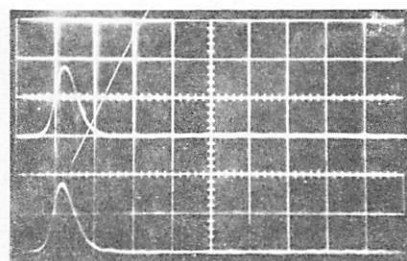




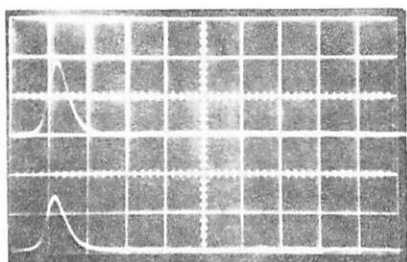
(a) No rod.



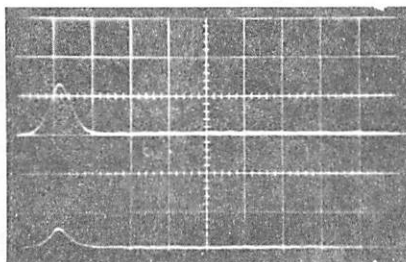
(b) Rod with 'c' axis aligned. (call it  $0^\circ$  position)



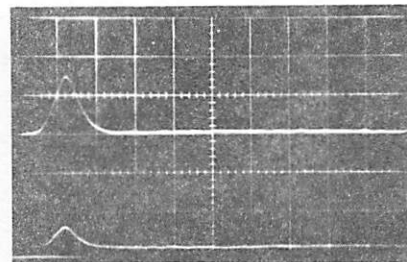
(c) Rotation of rod through  $22.5^\circ$



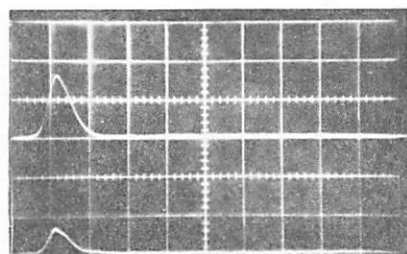
(d) Rotation of  $45^\circ$ .



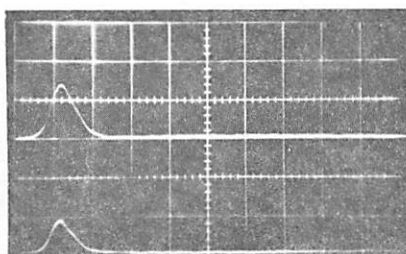
(e) Rotation of  $67.5^\circ$



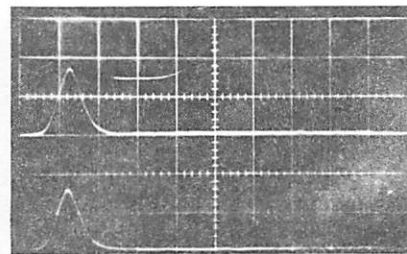
(f) Rotation of  $90^\circ$



(g) Rotation of  $112.5^\circ$

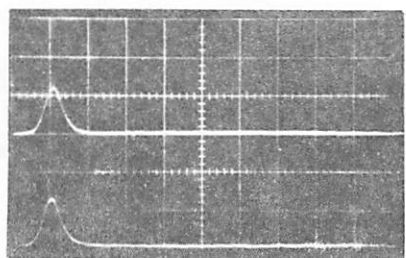


(h) Rotation of  $135^\circ$

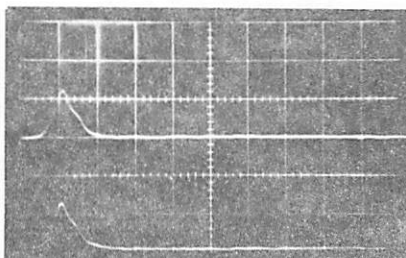


(i) Rotation of  $180^\circ$

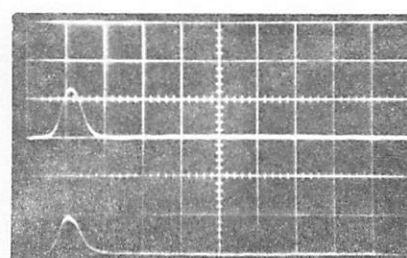
Fig. 8.  $90^\circ$  rotation of 'c' axis of the ruby. Firing voltage 3800 V. No filter at 'Q' spoiler.



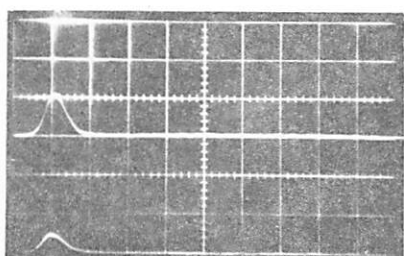
(a) No rod.



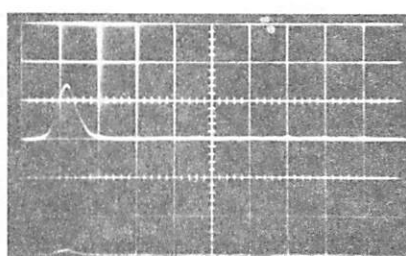
(b) Rod with 'c' axis aligned (call it  $0^\circ$  position).



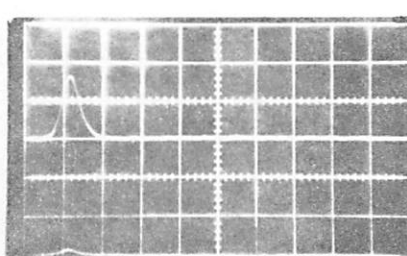
(c) Rotation of rod through  $22.5^\circ$ .



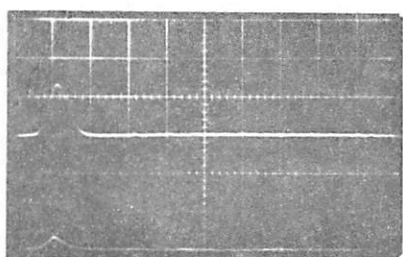
(d) Rotation of  $45^\circ$ .



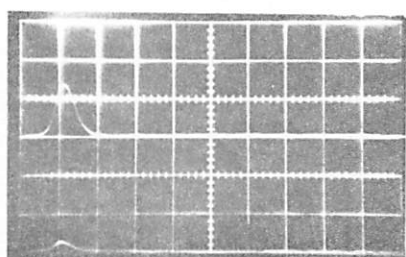
(e) Rotation of  $67.5^\circ$ .



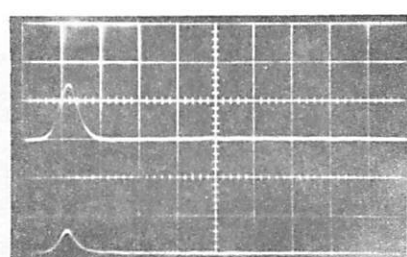
(f) Rotation of  $90^\circ$ .



(g) Rotation of  $112.5^\circ$ .

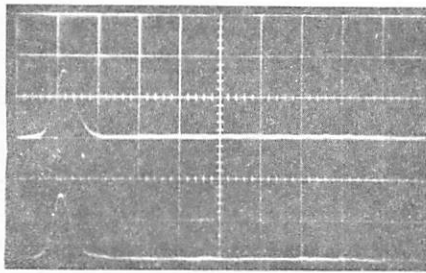


(h) Rotation of  $135^\circ$ .

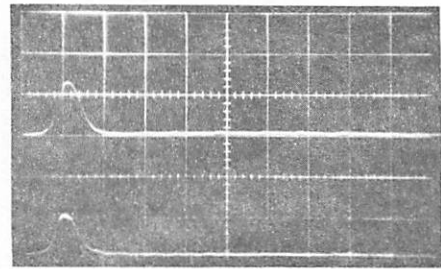


(i) Rotation of  $157.5^\circ$ .

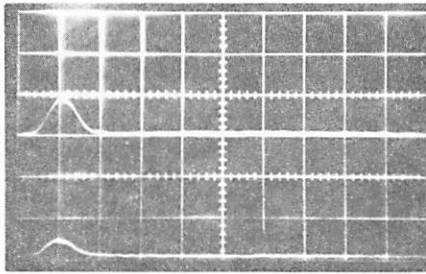
Fig. 9.  $90^\circ$  rotation of 'c' axis of ruby. Firing voltage 3800 V.  
N. D. 1.0 filter at 'Q' spoiler.



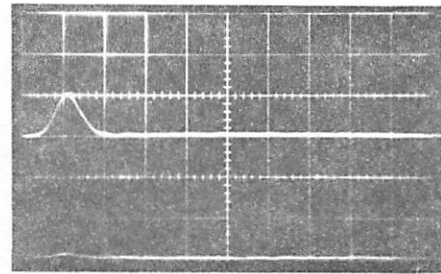
(a) Rod with 'c' axis aligned.  
(call it  $0^\circ$  position)



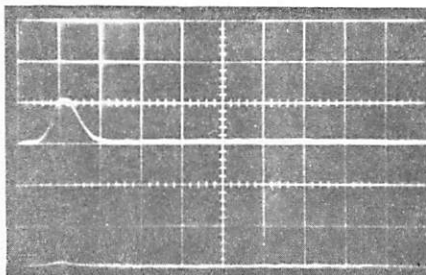
(b) Rotation of rod through  
 $22.5^\circ$ .



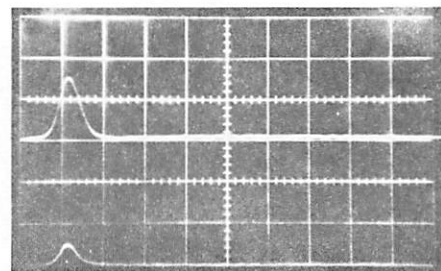
(c) Rotation of  $45^\circ$ .



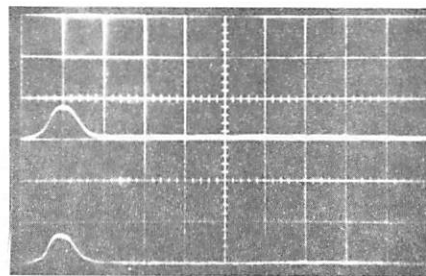
(d) Rotation of  $67.5^\circ$ .



(e) Rotation of  $90^\circ$ .



(f) Rotation of  $135^\circ$ .



(g) Rotation of  $180^\circ$ .

Fig. 10.  $90^\circ$  rotation of 'c' axis of ruby. Firing voltage 3800 V.  
N.D. 2.0 filter at 'Q' spoiler.

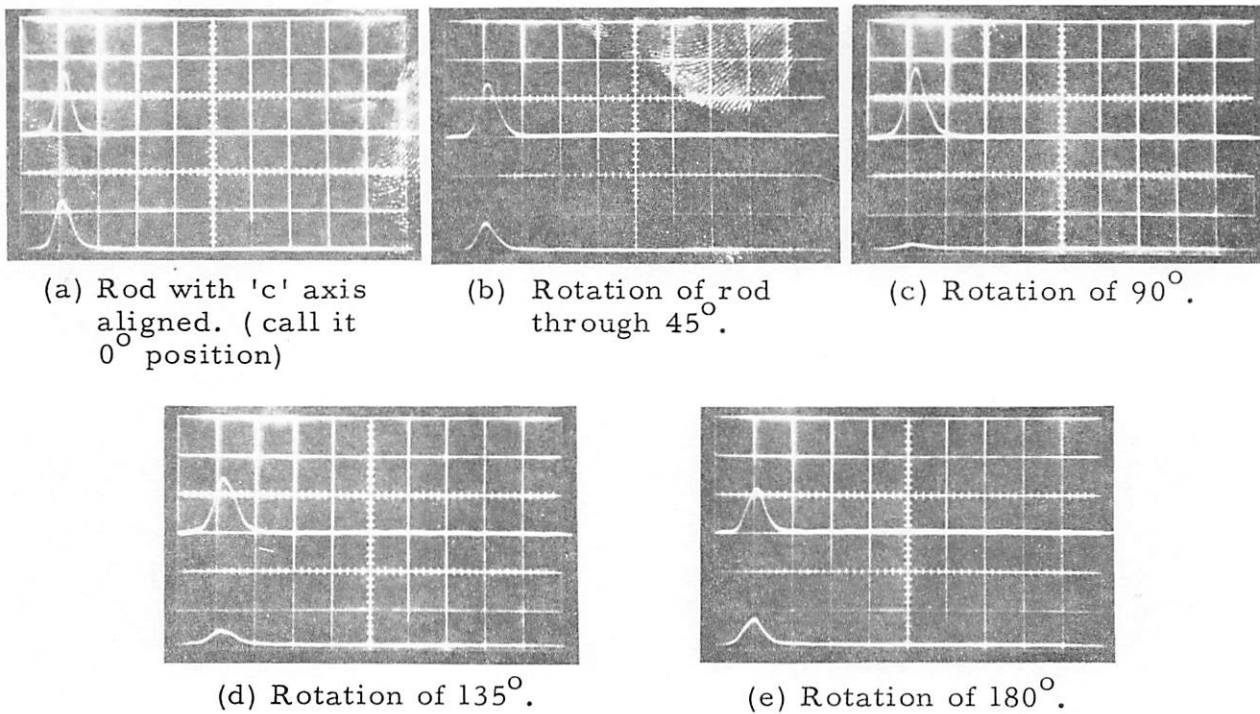


Fig. 11.  $90^\circ$  rotation of 'c' axis. Firing voltage 3800 V  
N. D. 4.0 filter at 'Q' spoiler.

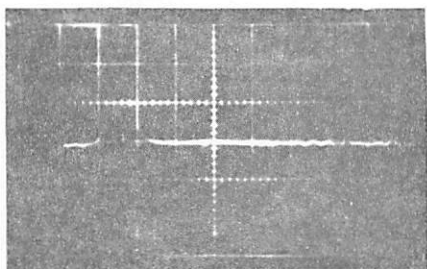


Fig. 12. Coated rod with  $0^\circ$  rotation of 'c' axis.  
Firing voltage 3800 V. No filter at 'Q' spoiler.

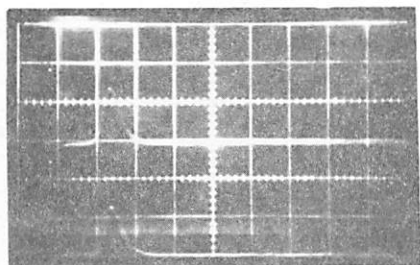


Fig. 13. Coated rod with  $90^\circ$  rotation of 'c' axis.  
Firing voltage 3800 V. No filter at 'Q' spoiler.

## REFERENCES

1. J. Weber, "Amplification of microwave radiation by substance not in thermal equilibrium," IRE Trans., Vol. ED-3, p. 1; 1953.
2. J. P. Gordon, H. J. Zeiger, and C. H. Townes, "Molecular microwave oscillator and new hyperfine structure in the microwave spectrum of  $\text{NH}_3$ ," Phys. Rev., Vol. 95, p. 282; 1954.  
                     \_\_\_\_\_, "The maser-new type of microwave amplifier, frequency standard and spectrometer," Ibid. Vol. 99, p. 1264; 1955.
3. A. L. Schawlow and C. H. Townes, "Infrared and optical masers," Ibid., Vol. 112, p. 1940; 1960.
4. T. H. Maiman, "Optical maser action in ruby," British Commun. and Electronics, Vol. 1, p. 674; 1960.  
                     \_\_\_\_\_, "Simulated optical radiation in ruby," Nature, Vol. 187, p. 493; 1960.
5. A. L. Schawlow, Quantum Electronics (C. H. Townes, Editor) Columbia University Press, New York, p. 533; 1960.
6. T. H. Maiman, et. al., "Stimulated optical emission in fluorescent solids. II. Spectroscopy and stimulated emission in ruby," Phys. Rev., Vol. 123, p. 1151; 1961.
7. S. Sugano and Y. Tanabe, "Absorption spectra of  $\text{Cr}^{3+}$  in  $\text{A}_2\text{O}_3$ ," J. Phys. Soc. Japan, Vol. 13, p. 880; 1958.
8. A. Yariv and J. P. Gordon, "The laser," Proc. IEEE, Vol. 51, p. 4; 1963.
9. J. R. Singer and S. Wang, "General analysis of optical infrared, and microwave maser oscillator emission," Phys. Rev. Lett., Vol. 6, pp. 351-355; 1961.

#### REFERENCES (Cont, d.)

10. S. Wang, and J. R. Singer, "Parametric maser oscillator analysis," J. Appl. Phys., Vol. 32, p. 1371; 1961.
11. See for example, J. R. Singer, Masers, John Wiley and Sons, Inc., New York; 1959.
12. See for example L. Pauling and E. Bright Wilson, Introduction to Quantum Mechanics, McGraw-Hill, Book Co., Inc., New York; 1935.
13. Communication from A. S. Pine.